The crystal structure and superconductivity of $(Pb_{0.5}Cd_{0.5})(Sr_{0.9}Ln_{0.1})_2(Ln_{0.7}Ce_{0.3})_2Cu_2O_9$ (Ln = Pr, Sm, Eu, Gd and Dy)

1996 J. Phys.: Condens. Matter 8 2869

(http://iopscience.iop.org/0953-8984/8/16/017)

J. Phys.: Condens. Matter **8** (1996) 2869–2879. Printed in the UK

The crystal structure and superconductivity of $(Pb_{0.5}Cd_{0.5})(Sr_{0.9}Ln_{0.1})_2(Ln_{0.7}Ce_{0.3})_2Cu_2O_9$ (Ln = Pr, Sm, Eu, Gd and Dy)

J R Min†, J K Liang†‡, C Wang†, C Dong§ and G H Rao†

† Institute of Physics, Chinese Academy of Sciences, Beijing 100080, People's Republic of China

‡ International Centre for Materials Physics, Academia Sinica, Shenyang 110015, People's Republic of China

§ National Laboratory for Superconductivity, Institute of Physics, Chinese Academy of Sciences, Beijing 100080, People's Republic of China

Received 11 December 1995

Abstract. In this paper we report the crystal structure and superconductivity of $(Pb_{0.5}Cd_{0.5})(Sr_{0.9}Ln_{0.1})_2(Ln_{0.7}Ce_{0.3})_2Cu_2O_9$ (Ln = Pr, Sm, Eu, Gd and Dy). The lattice parameters of these compounds decrease nearly linearly with the decrease of the average ionic radius of the rare-earth element (Ln, Ce), and the superconducting transition temperatures of these compounds increase as the ionic radius of the rare-earth element Ln decreases from Pr to Gd. $(Pb_{0.5}Cd_{0.5})(Sr_{0.9}Gd_{0.1})_2(Gd_{0.7}Ce_{0.3})_2Cu_2O_9$ has the highest T_c-values ($T_{c,\mathrm{onset}} = 49$ K, $T_{c,\mathrm{zero}} = 38$ K) which, to our knowledge, are also the highest T_c-values reported for any 1222 phase. The superconductivity of the system is affected by many factors: (i) the coupling effect between CuO_2 planes; (ii) the charge-carrier concentration in the CuO_2 planes; and (iii) the degree of buckling of CuO_2 planes.

1. Introduction

In 1986, Bednorz and Müller discovered the first high-temperature superconductor in the La–Ba–Cu–O system [1]. From then on, many other high-T_c copper oxides have been synthesized one after another. All of these copper oxides have a common structure feature, i.e., layered structure. The layered structures can be regarded as alternating stacks of different block layers, such as rock-salt-type layers, perovskite-type layers and/or fluorite-type layers. In general, those compounds containing fluorite-type layers have lower values of T_c than the corresponding compounds containing no fluorite-type layers. For example, the value of $T_{c,\mathrm{onset}}$ of Tl-1212 is about 100 K [2], while that of Tl-1222 is only about 40 K [3].

Following from the discovery of the first Pb-based superconducting copper oxide $Pb_2Sr_2ACu_3O_{8+\delta}$ (where A is a lanthanide or a mixture of Ln + Sr/Ca) by Cava *et al* [4], three kinds of Pb-based superconducting copper oxide have been discovered so far, i.e., (i) $(Pb_2Cu)(Sr, La)_2A_{n-1}Cu_nO_z$ (Pb-3201 ($n = 1$) and Pb-3212 ($n = 2$)) [4, 5] and $(Pb_2Cu)Sr_2(Ln, Ce)_nCu_2O_z$ (Pb-32n2, $n = 2, 3, 4, \ldots$) [6, 7] with PbO–Cu–PbO block layers; (ii) $(PbCu)(Ba, Sr)_2(Y, Ca)Cu_2O_7$ (Pb-2212) [8] and $(PbCu)(Ba, Sr)_2(Ln, Ce)_nCu_2O_z$ (Pb-22n2, $n = 2, 3, 4, \ldots$) [7, 9] with PbO–CuO_x block layers; and lastly (iii) $(Pb, M)(Sr, La)_2(Y, Ca)_{n-1}Cu_nO_z$ (Pb-1201 ($n = 1$), Pb-1212 ($n = 2$)) [10–13] with

0953-8984/96/162869+11$19.50

(Pb, M)O block layers (M = divalent metal element, such as Cu and Cd). Adachi *et al* discovered the first non-superconducting Pb-1222 phase $(Pb, Cu)(Sr, Pr)_2Pr_2Cu_2O_9$ in 1990 [14]. The crystal structure of the (Pb, Cu)-1222 phase is derived from that of $(Pb, Cu)Sr_2(Y, Ca)Cu_2O_9$ with an oxygen-deficient (Y, Ca) layer replaced by a fluorite-type $(Ln, Ce)_2O_2$ layer. Careful research has since been carried out on the system $(Pb, Cu)(Sr, Ln)_2(Ln, Ce)_2Cu_2O_9$ (Ln = lanthanide element), and a series of superconducting (Pb, Cu)-1222 compounds have been obtained [15–17]. Up to the present, the highest value of $T_{c,\mathrm{onset}}$ of 32 K was reported for $(Pb_{0.5}Cu_{0.5})(Sr_{7/8}Nd_{1/8})_2(Eu_{3/4}Ce_{1/4})_2Cu_2O_9$ (see [16]). In this paper, we report on another series of superconducting copper oxides $(Pb_{0.5}Cd_{0.5})(Sr_{0.9}Ln_{0.1})_2(Ln_{0.7}Ce_{0.3})_2Cu_2O_9$ (Ln = Pr, Sm, Eu, Gd and Dy), among which $(Pb_{0.5}Cd_{0.5})(Sr_{0.9}Gd_{0.1})_2(Gd_{0.7}Ce_{0.3})_2Cu_2O_9$ has the highest T_c-values ($T_{c,\mathrm{onset}}$ = 49 K, $T_{c,\mathrm{zero}}$ = 38 K). To our knowledge, these values are also the highest T_c-values observed for any 1222 phase. Besides this, we study the effect of the rare-earth element Ln on the crystal structure and superconductivity of $(Pb_{0.5}Cd_{0.5})(Sr_{0.9}Ln_{0.1})_2(Ln_{0.7}Ce_{0.3})_2Cu_2O_9$ (Ln = Pr, Sm, Eu, Gd and Dy).

2. Experimental procedure

Samples with a nominal composition of $(Pb_{0.5}Cd_{0.5})(Sr_{0.9}Ln_{0.1})_2(Ln_{0.7}Ce_{0.3})_2Cu_2O_9$ (Ln = La, Ce, Pr, Nd, Sm, Eu, Gd, Tb, Dy, Y and Er) were prepared by the solid-state reaction method using PbO, CdO, $SrCO_3$, La_2O_3, CeO_2, Pr_6O_{11}, Nd_2O_3, Sm_2O_3, Eu_2O_3, Gd_2O_3, TbO_2, Dy_2O_3, Y_2O_3, Er_2O_3 and CuO as starting materials. Stoichiometric amounts of starting materials were appropriately weighted, and ground together in an agate mortar. The well mixed powders were calcined at 900 °C in air overnight and then furnace cooled to room temperature. The prereacted material was reground and pressed into pellets. The pellets were sintered at 1050 °C in air for eight hours. Finally, the pellets were ground once more, and then pressed and sintered at 1050 °C in air and flowing O_2, respectively.

X-ray powder diffraction (XRD) analyses were performed on an M18AHF x-ray diffractometer with Cu Kα radiation (50 kV × 200 mA). The structure refinement data were collected on the same diffractometer at ambient temperature. The scattering slit is 0.50°, the divergence slit 0.50°, and the receiving slit 0.15 mm. The scanning step width is 0.02° in 2θ and the sampling time is 2 s per step. The 2θ-range is from 10 to 110°. A standard four-probe method was used for electrical resistivity measurements.

3. Results

3.1. Synthesis and superconductivity

A series of samples in the $(Pb_{0.5}Cd_{0.5})(Sr_{0.9}Ln_{0.1})_2(Ln_{0.7}Ce_{0.3})_2Cu_2O_9$ system (Ln = La, Ce, Pr, Nd, Sm, Eu, Gd, Tb, Dy, Y and Er) have been prepared. The phase identification results indicate that nearly single-phase (Pb, Cd)-1222 phase can be obtained for Ln = Pr, Sm, Eu and Gd. A small amount of impurity phase exists in the Ln = Dy sample. Figure 1 shows the x-ray powder diffraction patterns of $(Pb_{0.5}Cd_{0.5})(Sr_{0.9}Ln_{0.1})_2(Ln_{0.7}Ce_{0.3})_2Cu_2O_9$ (Ln = Pr, Sm, Eu, Gd, and Dy). $(Pb_{0.5}Cd_{0.5})(Sr_{0.9}Ln_{0.1})_2(Ln_{0.7}Ce_{0.3})_2Cu_2O_9$ is very sensitive to sintering temperature and atmosphere. Inappropriate synthesis conditions can lead to the appearance of impurity phases, because the components of our Pb-1222 phases are very complex and some of them can form Pb-1212 phase or 214 phase. The optimal synthesis conditions for the present Pb-1222 are sintering at 1050 °C in an oxidizing atmosphere (air or O_2).

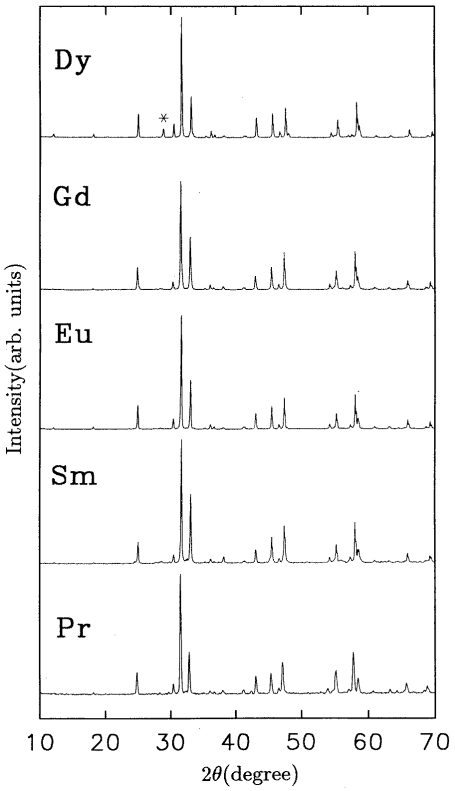

Figure 1. X-ray powder diffraction patterns for $(Pb_{0.5}Cd_{0.5})(Sr_{0.9}Ln_{0.1})_2(Ln_{0.7}Ce_{0.3})_2Cu_2O_9$ (Ln = Pr, Sm, Eu, Gd, and Dy).

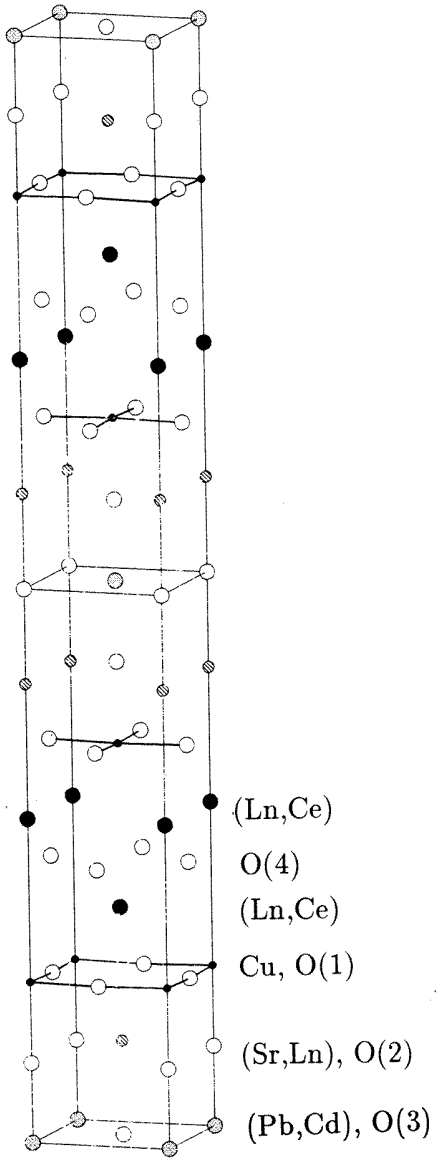

Figure 2. A schematic representation of the crystal structure of $(Pb, Cd)(Sr, Ln)_2(Ln, Ce)_2Cu_2O_9$.

We have listed in table 1 the superconducting transition temperatures of $(Pb_{0.5}Cd_{0.5})(Sr_{0.9}Ln_{0.1})_2(Ln_{0.7}Ce_{0.3})_2Cu_2O_9$ (Ln = Pr, Sm, Eu, Gd and Dy), measured by electrical resistivity. It can be seen from table 1 that the T_c-values of these samples are closely correlated with the choice of rare-earth element Ln and the sintering atmosphere. The superconducting transition temperatures of these samples increase as the ionic radius of the rare-earth element Ln decreases, from Pr to Gd.

Table 1. Superconducting transition temperatures $T_{c,\mathrm{onset}}$, $T_{c,\mathrm{zero}}$ and conducting behaviour for $(Pb_{0.5}Cd_{0.5})(Sr_{0.9}Ln_{0.1})_2(Ln_{0.7}Ce_{0.3})_2Cu_2O_z$ (Ln = Pr, Sm, Eu, Gd, and Dy).

Composition and sintering atmosphere	$T_{c,\mathrm{onset}}$	$T_{c,\mathrm{zero}}$	Conducting behaviour
$(Pb_{0.5}Cd_{0.5})(Sr_{0.9}Pr_{0.1})_2(Pr_{0.7}Ce_{0.3})_2Cu_2O_z$, O_2	<4.2 K	<4.2 K	Semiconductor
$(Pb_{0.5}Cd_{0.5})(Sr_{0.9}Sm_{0.1})_2(Sm_{0.7}Ce_{0.3})_2Cu_2O_z$, O_2	41 K	29 K	Semiconductor
$(Pb_{0.5}Cd_{0.5})(Sr_{0.9}Eu_{0.1})_2(Eu_{0.7}Ce_{0.3})_2Cu_2O_z$, O_2	43 K	35 K	Metal
$(Pb_{0.5}Cd_{0.5})(Sr_{0.9}Gd_{0.1})_2(Gd_{0.7}Ce_{0.3})_2Cu_2O_z$, O_2	49 K	38 K	Metal
$(Pb_{0.5}Cd_{0.5})(Sr_{0.9}Dy_{0.1})_2(Dy_{0.7}Ce_{0.3})_2Cu_2O_z$, O_2	12 K	<4.2 K	Semiconductor
$(Pb_{0.5}Cd_{0.5})(Sr_{0.9}Eu_{0.1})_2(Eu_{0.7}Ce_{0.3})_2Cu_2O_z$, air	19 K	12 K	Semiconductor
$(Pb_{0.5}Cd_{0.5})(Sr_{0.9}Gd_{0.1})_2(Gd_{0.7}Ce_{0.3})_2Cu_2O_z$, air	29 K	20 K	Semiconductor

$(Pb_{0.5}Cd_{0.5})(Sr_{0.9}Gd_{0.1})_2(Gd_{0.7}Ce_{0.3})_2Cu_2O_9$ has the highest T_c-values ($T_{c,\mathrm{onset}}$ = 49 K, $T_{c,\mathrm{zero}}$ = 38 K) which, to our knowledge, are also the highest T_c-values reported for any 1222 phase. Besides this, the O_2-synthesized $(Pb_{0.5}Cd_{0.5})(Sr_{0.9}Ln_{0.1})_2(Ln_{0.7}Ce_{0.3})_2Cu_2O_9$ samples (Ln = Gd and Eu) exhibit a metallic behaviour in their normal state, while the air-synthesized $(Pb_{0.5}Cd_{0.5})(Sr_{0.9}Ln_{0.1})_2(Ln_{0.7}Ce_{0.3})_2Cu_2O_9$ samples (Ln = Gd and Eu) exhibit a semiconducting behaviour in their normal state. This is a typical metal–insulator transition with the increase of the carrier concentration. However, the O_2-synthesized $(Pb_{0.5}Cd_{0.5})(Sr_{0.9}Ln_{0.1})_2(Ln_{0.7}Ce_{0.3})_2Cu_2O_9$ samples (Ln = Sm and Dy) exhibit a semiconducting behaviour in their normal state. Thus, both the rare-earth element Ln and the sintering atmosphere can affect the superconducting transition temperatures and the conducting behaviour of these samples, which will be discussed in section 4 in detail.

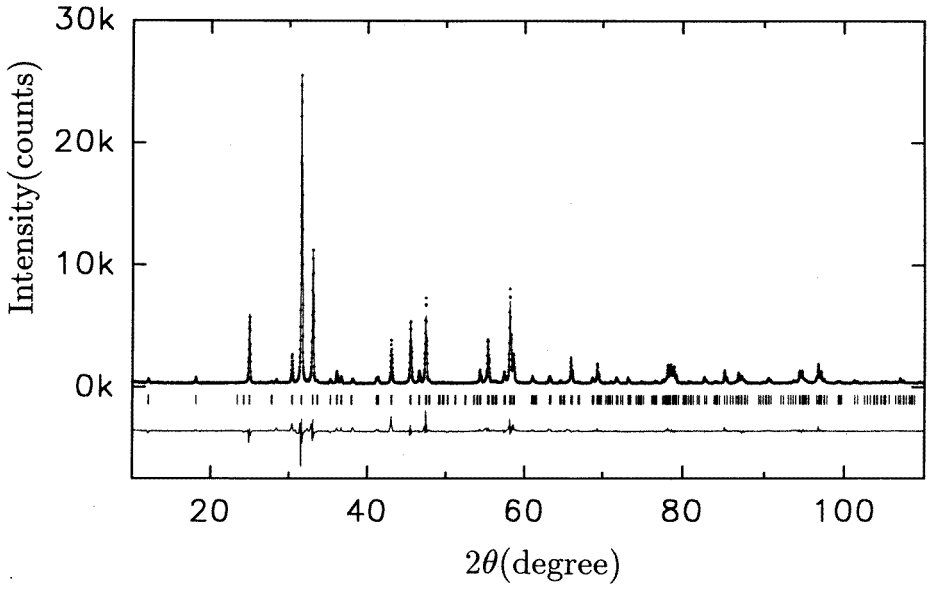

Figure 3. The Rietveld refinement pattern for $(Pb_{0.5}Cd_{0.5})(Sr_{0.9}Eu_{0.1})_2(Eu_{0.7}Ce_{0.3})_2Cu_2O_9$.

Table 2. Refined structure parameters from powder x-ray Rietveld analysis for the compounds $(Pb_{0.5}Cd_{0.5})(Sr_{0.9}Ln_{0.1})_2(Ln_{0.7}Ce_{0.3})_2Cu_2O_9$ (Ln = Pr, Sm, Eu, Gd and Dy). Space group: $I4/mmm$. $Z = 2$. The ratio of Pb and Cd in the (Pb, Cd)O layers is fixed at 0.5:0.5. The ratio of Sr and Ln at the 4e site in the (Sr, Ln)O layers is fixed at 0.9:0.1. The ratio of Ln and Ce at the 4e site in the $(Ln, Ce)_2O_2$ layers is fixed at 0.7:0.3. The numbers in parentheses are estimated standard deviations of the last significant digit, and those without deviations were fixed. B is the isotropic temperature factor with a unit of Å^2.

Atom	Site		Pr*	Sm*	Eu(O_2)*	Eu(air)*	Gd*	Dy*
(Pb, Cd)	8i	(x)	0.049(3)	0.071(2)	0.068(1)	0.054(3)	0.056(2)	0.057(3)
		(B)	0.35(8)	0.56(3)	0.23(3)	0.51(2)	0.56(4)	0.50(3)
		(g)	0.25	0.25	0.25	0.25	0.25	0.25
(Sr, Ln)	4e	(z)	0.0843(2)	0.0850(2)	0.0853(1)	0.0848(1)	0.0854(2)	0.0856(2)
		(B)	0.33(3)	0.48(3)	0.33(3)	0.17(2)	0.48(2)	0.39(5)
		(g)	1	1	1	1	1	1
(Ln, Ce)	4e	(z)	0.2057(1)	0.2065(1)	0.2067(1)	0.2066(1)	0.2069(3)	0.2072(1)
		(B)	0.28(2)	0.52(1)	0.41(4)	0.42(3)	0.22(3)	0.32(1)
		(g)	1	1	1	1	1	1
Cu	4e	(z)	0.1444(3)	0.1456(3)	0.1463(2)	0.1468(3)	0.1467(2)	0.1474(3)
		(B)	0.17(2)	0.22(1)	0.19(1)	0.27(1)	0.28(3)	0.32(1)
		(g)	1	1	1	1	1	1
O(1)	8g	(z)	0.1401(9)	0.1431(5)	0.1449(5)	0.1447(8)	0.1465(6)	0.1507(7)
		(g)	1	1	1	1	1	1
O(2)	4e	(z)	0.0703(10)	0.0723(7)	0.0726(6)	0.0722(9)	0.0740(7)	0.0745(9)
		(g)	1	1	1	1	1	1
O(3)	8j	(x)	0.36(2)	0.49(4)	0.457(9)	0.452(2)	0.49(8)	0.40(2)
		(g)	0.25	0.25	0.25	0.25	0.25	0.25
O(4)	4d	(g)	1	1	1	1	1	1
a (Å)			3.8702(6)	3.8351(5)	3.8314(3)	3.8443(4)	3.8224(3)	3.8133(4)
c (Å)			29.5008(5)	29.4334(4)	29.3902(20)	29.3937(11)	29.3538(27)	29.2892(14)
R_p (%)			8.01	9.34	7.63	9.50	7.86	8.94
R_{wp} (%)			11.27	13.72	10.25	13.31	10.60	12.83

Pr: $(Pb_{0.5}Cd_{0.5})(Sr_{0.9}Pr_{0.1})_2(Pr_{0.7}Ce_{0.3})_2Cu_2O_9$, synthesized in O_2

Sm: $(Pb_{0.5}Cd_{0.5})(Sr_{0.9}Sm_{0.1})_2(Sm_{0.7}Ce_{0.3})_2Cu_2O_9$, synthesized in O_2

Eu(O_2): $(Pb_{0.5}Cd_{0.5})(Sr_{0.9}Eu_{0.1})_2(Eu_{0.7}Ce_{0.3})_2Cu_2O_9$, synthesized in O_2

Eu(air): $(Pb_{0.5}Cd_{0.5})(Sr_{0.9}Eu_{0.1})_2(Eu_{0.7}Ce_{0.3})_2Cu_2O_9$, synthesized in air

Gd: $(Pb_{0.5}Cd_{0.5})(Sr_{0.9}Gd_{0.1})_2(Gd_{0.7}Ce_{0.3})_2Cu_2O_9$, synthesized in O_2

Dy: $(Pb_{0.5}Cd_{0.5})(Sr_{0.9}Dy_{0.1})_2(Dy_{0.7}Ce_{0.3})_2Cu_2O_9$, synthesized in O_2

3.2. Crystal structure

The crystal structure of $(Pb, Cu)(Sr, Nd)_2(Ho, Ce)_2Cu_2O_{9.06}$ has been reported by Maeda *et al* [17]. According to this structure model, we have refined the structure parameters of $(Pb_{0.5}Cd_{0.5})(Sr_{0.9}Ln_{0.1})_2(Ln_{0.7}Ce_{0.3})_2Cu_2O_9$ (Ln = Pr, Sm, Eu, Gd and Dy) by the Rietveld method [18] using x-ray powder diffraction data. Figure 2 shows the schematic representation of the crystal structure of $(Pb, Cd)(Sr, Ln)_2(Ln, Ce)_2Cu_2O_9$. There are four different crystallographic sites for the metal atoms in the present Pb-1222 phase. It is supposed that Sr^{2+} and Ce^{4+} occupy different crystallographic sites because of the large difference in their ionic radii [19]. Larger Sr^{2+} is assumed to selectively occupy the 9-coordinated site in the rock-salt-type layers, while smaller Ce^{4+} is assumed to occupy

Table 3. Selected metal–oxygen interatomic distances and bond valence sums of Cu ions in the CuO_2 planes for $(Pb_{0.5}Cd_{0.5})(Sr_{0.9}Ln_{0.1})_2(Ln_{0.7}Ce_{0.3})_2Cu_2O_9$ (Ln = Pr, Sm, Eu, Gd and Dy). For the sake of convenience, the displaced atoms were placed at their ideal positions while calculating the (Pb, Cd)–O(3) distance. N is the number of equivalent bonds.

Bonds	Pr*	Sm*	Eu(O_2)*	Eu(air)*	Gd*	Dy*	N
(Pb, Cd)–O(2)	2.083	2.145	2.150	2.131	2.183	2.193	2
(Pb, Cd)–O(3)	2.737	2.712	2.709	2.718	2.703	2.696	4
(Sr, Ln)–O(1)	2.541	2.569	2.595	2.606	2.621	2.696	4
(Sr, Ln)–O(2)	2.768	2.737	2.735	2.744	2.723	2.716	4
(Sr, Ln)–O(3)	2.545	2.502	2.514	2.500	2.507	2.536	1
(Ln, Ce)–O(1)	2.737	2.676	2.639	2.648	2.607	2.525	4
(Ln, Ce)–O(4)	2.335	2.306	2.301	2.306	2.292	2.282	4
Cu–O(1)	1.939	1.919	1.916	1.923	1.911	1.909	4
Cu–O(2)	2.186	2.157	2.164	2.195	2.134	2.135	1
	Bond valence sums						
Cu	2.39	2.63	2.65	2.53	2.75	2.77	

Pr: $(Pb_{0.5}Cd_{0.5})(Sr_{0.9}Pr_{0.1})_2(Pr_{0.7}Ce_{0.3})_2Cu_2O_9$, synthesized in O_2

Sm: $(Pb_{0.5}Cd_{0.5})(Sr_{0.9}Sm_{0.1})_2(Sm_{0.7}Ce_{0.3})_2Cu_2O_9$, synthesized in O_2

Eu(O_2): $(Pb_{0.5}Cd_{0.5})(Sr_{0.9}Eu_{0.1})_2(Eu_{0.7}Ce_{0.3})_2Cu_2O_9$, synthesized in O_2

Eu(air): $(Pb_{0.5}Cd_{0.5})(Sr_{0.9}Eu_{0.1})_2(Eu_{0.7}Ce_{0.3})_2Cu_2O_9$, synthesized in air

Gd: $(Pb_{0.5}Cd_{0.5})(Sr_{0.9}Gd_{0.1})_2(Gd_{0.7}Ce_{0.3})_2Cu_2O_9$, synthesized in O_2

Dy: $(Pb_{0.5}Cd_{0.5})(Sr_{0.9}Dy_{0.1})_2(Dy_{0.7}Ce_{0.3})_2Cu_2O_9$, synthesized in O_2

the 8-coordinated site in the fluorite-type layers. Ln^{3+} is assumed to be distributed to the two sites (see figure 2). The occupancy refinements of (Pb, Cd)O layers, (Sr, Ln)O layers, $(Ln, Ce)_2O_2$ layers and CuO_2 planes indicate that the compositions in these layers are almost stoichiometric. Thus, these values are fixed at their nominal compositions in the final refinement. The thermal parameters (B) are assumed to be isotropic, and the thermal parameters of all oxygen atoms are arbitrarily fixed at 1 $Å^2$. Table 2 lists the final R-factors, the refined lattice constants, structure parameters and their estimated standard deviations in parentheses for $(Pb_{0.5}Cd_{0.5})(Sr_{0.9}Ln_{0.1})_2(Ln_{0.7}Ce_{0.3})_2Cu_2O_9$ (Ln = Pr, Sm, Eu, Gd and Dy). Table 3 lists the selected metal–oxygen interatomic distances for these samples. Figure 3 shows the Rietveld refinement pattern for the O_2-synthesized $(Pb_{0.5}Cd_{0.5})(Sr_{0.9}Eu_{0.1})_2(Eu_{0.7}Ce_{0.3})_2Cu_2O_9$ as an example. The dotted line represents the observed diffraction pattern, the solid line represents the calculated pattern, and the curve at the bottom represents the difference between the observed and calculated patterns. The short vertical lines mark the positions of possible Bragg reflections for the (Pb, Cd)-1222 phase. The remarkably good fit between the observed and calculated patterns supports the suggested structure model.

According to the bond valence model advanced by Brown *et al* (see [19]), the atomic valence of an atom is assumed to be distributed between the bonds it forms. As a result, the atomic valence V_i is obtained by summing up the valences of the bonds formed by atom i

given by

$$V_i = \sum_j S_{ij} \tag{1}$$

where S_{ij} is the valence of the bond between atoms i and j. The usefulness of this rule lies in the correlation observed between the length (R) and the valence (S_{ij}) of a bond as expressed by

$$S_{ij} = \exp((R_0 - R)/B) \tag{2}$$

where $B = 0.37$ Å and R_0 represents the length of the bond between atoms i and j of unit valence. Because R_0 depends on oxidation state, the oxidation states of the Cu atoms must be known before the bond valences can be calculated. However, the bond valences are needed in order to determine the oxidation states. This problem has been solved using the procedure developed by Brown [19]. Valences (S_{ij}) were calculated assuming that the copper was Cu^{2+}. Then the bond valence sum ($V_{2+} = \sum S_{ij}$) around a Cu atom was used to determine whether its oxidation state was greater than or less than 2. Generally, the oxidation state of Cu ions in the hole-type superconducting copper oxides is greater than +2. In this case, the proportion (y) of Cu^{3+} was calculated using the equation

$$y = (V_{2+} - 2)/(V_{2+} + 1.0 - V_{3+}) \tag{3}$$

where V_{2+} is the bond valence sum calculated by assuming that the copper is Cu^{2+} and V_{3+} is the bond valence sum calculated by assuming that the copper is Cu^{3+}. The values of R_0 for Cu^{2+}–O^{2-} and Cu^{3+}–O^{2-} are 1.679 Å and 1.739 Å, respectively.

The bond valence sums of Cu ions in the conducting CuO_2 planes for the compounds $(Pb_{0.5}Cd_{0.5})(Sr_{0.9}Ln_{0.1})_2(Ln_{0.7}Ce_{0.3})_2Cu_2O_9$ (Ln = Pr, Sm, Eu, Gd and Dy) have been calculated using the above procedure and are listed in table 3.

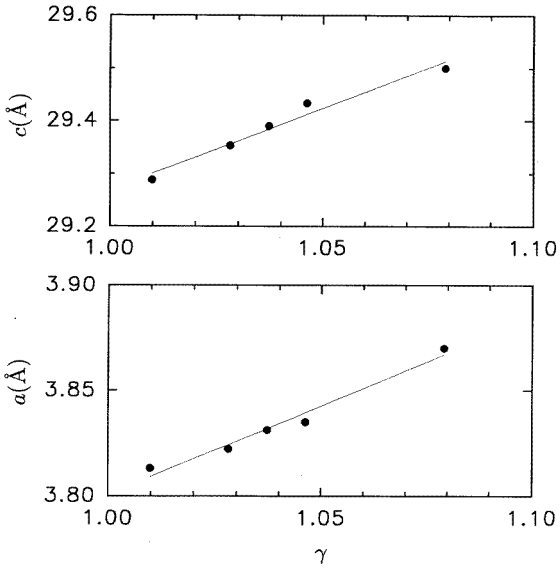

Figure 4. The variations of the lattice parameters a and c with the average ionic radii γ of the rare-earth element (Ln, Ce) in the $(Pb_{0.5}Cd_{0.5})(Sr_{0.9}Ln_{0.1})_2(Ln_{0.7}Ce_{0.3})_2Cu_2O_9$ system. $\gamma = 0.7\gamma_{Ln^{3+}} + 0.3\gamma_{Ce^{4+}}$, CN = 8.

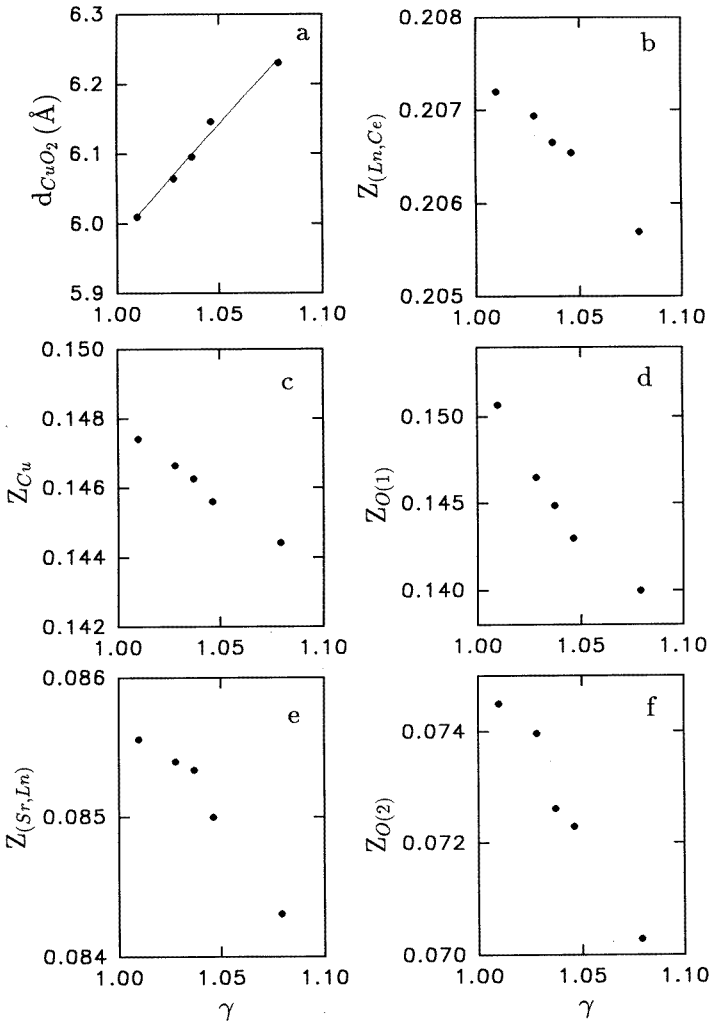

Figure 5. The variations of the interplanar distance between adjacent CuO_2 planes and the positional parameters with the average ionic radius γ of the rare-earth element (Ln, Ce). $\gamma = 0.7\gamma_{Ln^{3+}} + 0.3\gamma_{Ce^{4+}}$, CN = 8.

4. Discussion

The lattice parameters of $(Pb_{0.5}Cd_{0.5})(Sr_{0.9}Ln_{0.1})_2(Ln_{0.7}Ce_{0.3})_2Cu_2O_9$ (Ln = Pr, Sm, Eu, Gd and Dy) have been accurately determined by the Rietveld refinement. Figure 4 shows the variations of the lattice parameters a and c with the average ionic radius γ of the (Ln, Ce) site ($\gamma = 0.7\gamma_{Ln^{3+}} + 0.3\gamma_{Ce^{4+}}$, CN = 8) in the $(Pb_{0.5}Cd_{0.5})(Sr_{0.9}Ln_{0.1})_2(Ln_{0.7}Ce_{0.3})_2Cu_2O_9$ system. It can be seen from the figure that, for the present (Pb, Cd)-1222 system, the lattice parameters decrease nearly linearly with the decrease of the average ionic radius of the rare-earth element (Ln, Ce). This indicates that the crystal structure of the present compounds is very rigid. Besides this, it can be expected that the interplanar distance between adjacent CuO_2 planes will expand as the average ionic radius of the rare-earth element (Ln, Ce)

increases. Figure 5(a) shows the variation of the interplanar distance between adjacent CuO_2 planes with the average ionic radius of the rare-earth element (Ln, Ce). The interplanar distance between adjacent CuO_2 planes changes linearly with the average ionic radius of the rare-earth elements (Ln, Ce). Furthermore, it can also be reasonably concluded that the increase of the average ionic radius of the rare-earth element (Ln, Ce) will lead to the decrease of the positional parameters $Z_{(Ln,\,Ce)}$, Z_{Cu}, $Z_{O(1)}$, $Z_{(Sr,\,Ln)}$, and $Z_{O(2)}$. Figures 5(b)–5(f) show the variations of these positional parameters with the average ionic radius of the rare-earth element (Ln, Ce).

In general, it is thought that the effect of coupling between adjacent CuO_2 planes is a crucial factor in controlling the superconductivity of high-T_c copper oxides. The coupling between adjacent CuO_2 planes strengthens as the interplanar distance between adjacent CuO_2 planes decreases. In the $(Pb_{0.5}Cd_{0.5})(Sr_{0.9}Ln_{0.1})_2(Ln_{0.7}Ce_{0.3})_2Cu_2O_9$ (Ln = Pr, Sm, Eu, Gd and Dy) system, the decrease of the ionic radius of the rare-earth element Ln leads to a decrease of the interplanar distance between adjacent CuO_2 planes. Consequently, it strengthens the coupling between CuO_2 planes, which will be beneficial as regards improving the superconductivity of the present (Pb, Cd)-1222 phase. The T_c-values for these (Pb, Cd)-1222 compounds have been listed in table 1. It can be seen from this table that, from Pr to Gd, with the decrease of the ionic radius of the rare-earth element the T_c-values undergo an evident increase. At the same time, the conducting behaviour also undergoes a corresponding change. The (Pb, Cd)-1222 compounds containing larger Ln exhibit a semiconducting behaviour, while the (Pb, Cd)-1222 compounds containing smaller Ln exhibit a metal-type behaviour when synthesized in O_2. The effect of the coupling between adjacent CuO_2 planes can be more clearly seen from the fact that the superconductivity of all high-T_c oxide superconductors deteriorates when their oxygen-deficient (Y, Ca) layers are replaced by Ln_2O_2 layers. For example, Tl-1212 has a value of $T_{c,\mathrm{onset}}$ of about 100 K [2], while Tl-1222 has a value of $T_{c,\mathrm{onset}}$ of only about 40 K [3]. The Ln = Dy compound just exhibits weak superconductivity, and zero resistance is not achieved until 4.2 K is reached. It is suggested that one possible reason for the weak superconductivity of the Ln = Dy sample may be the appearance of the impurity phase (see figure 1). Other possible reasons will be discussed below.

Table 4. Bond angles of Cu–O(1)–Cu for $(Pb_{0.5}Cd_{0.5})(Sr_{0.9}Ln_{0.1})_2(Ln_{0.7}Ce_{0.3})_2Cu_2O_9$ (Ln = Pr, Sm, Eu, Gd and Dy) synthesized at 1050 °C in flowing O_2.

Sample	Composition	Cu–O(1)–Cu (deg)	T_c (K)
Pr	$(Pb_{0.5}Cd_{0.5})(Sr_{0.9}Pr_{0.1})_2(Pr_{0.7}Ce_{0.3})_2Cu_2O_9$	172.50	<4.2 K
Sm	$(Pb_{0.5}Cd_{0.5})(Sr_{0.9}Sm_{0.1})_2(Sm_{0.7}Ce_{0.3})_2Cu_2O_9$	175.60	41 K
Eu	$(Pb_{0.5}Cd_{0.5})(Sr_{0.9}Eu_{0.1})_2(Eu_{0.7}Ce_{0.3})_2Cu_2O_9$	177.54	43 K
Gd	$(Pb_{0.5}Cd_{0.5})(Sr_{0.9}Gd_{0.1})_2(Gd_{0.7}Ce_{0.3})_2Cu_2O_9$	179.64	49 K
Dy	$(Pb_{0.5}Cd_{0.5})(Sr_{0.9}Dy_{0.1})_2(Dy_{0.7}Ce_{0.3})_2Cu_2O_9$	174.20	12 K

Besides the coupling effect between adjacent CuO_2 planes, the charge-carrier concentration in the CuO_2 planes also plays an important role in the superconductivity of high-T_c copper oxides. For high-T_c layered copper oxides, the lattice parameter a is mainly decided by Cu–O bond length, which reflects the valence state of the Cu ions. It can be seen from figure 5 that, as the ionic radius of the rare-earth element Ln decreases, from Pr^{3+} to Dy^{3+}, the a-value decreases. Comparing the (Ln, Ce)–O(4) bond length (about 2.3 Å; see table 4) with the ideal interatomic distance between (Ln, Ce) and O(4) from ionic radius considerations (about 2.5 Å), it is found that the (Ln, Ce)–O(4) bond should be in a

compressed state, while the Cu–O(1) bond should be in a tensile state. Thus, the decrease of the ionic radius of the rare-earth element Ln will shorten the length of both the (Ln, Ce)–O(4) bond and the Cu–O(1) bond. This can be seen clearly from table 3. Therefore, as the ionic radius of the rare-earth element Ln decreases, the valence states of the Cu ions in the conducting CuO_2 planes in these compounds increase, which is proved by our calculations of the bond valence sums of the Cu ions in the CuO_2 plane (table 3). So the compounds containing the smaller rare-earth element Ln should have higher carrier concentration and better superconductivity.

Furthermore, the degree of buckling of CuO_2 planes can also affect the superconductivity of high-T_c copper oxides. It has been shown fairly clearly using high-pressure methods that for the $La_{2-x}Sr_xCuO_4$ system, flat layers result in marginally higher values of T_c [20, 21]. Table 4 lists the degrees of buckling of the CuO_2 planes for the system $(Pb_{0.5}Cd_{0.5})(Sr_{0.9}Ln_{0.1})_2(Ln_{0.7}Ce_{0.3})_2Cu_2O_9$ (Ln = Pr, Sm, Eu, Gd and Dy). It can be seen from table 4 that, going from Pr to Gd, the CuO_2 planes become flatter and flatter and the T_c-values of the corresponding samples increase. On the other hand, however, the degree of buckling of the CuO_2 planes for the Ln = Dy sample begins to increase, and the sample shows weak superconductivity. Thus, this trend in the variation of the degrees of buckling of the CuO_2 planes in this system is in good agreement with the T_c-values of the samples. This is further evidence that the degree of buckling of CuO_2 planes can affect the superconductivity of high-T_c copper oxides, and also another reason for which the Ln = Dy sample just exhibits weak superconductivity.

From table 3, it is found that the bond valence sums of the Cu ions in the O_2-synthesized $(Pb_{0.5}Cd_{0.5})(Sr_{0.9}Eu_{0.1})_2(Eu_{0.7}Ce_{0.3})_2Cu_2O_9$ are higher than those in the air-synthesized $(Pb_{0.5}Cd_{0.5})(Sr_{0.9}Eu_{0.1})_2(Eu_{0.7}Ce_{0.3})_2Cu_2O_9$. This indicates that the O_2-synthesized sample has higher carrier concentration than the air-synthesized sample, which is consistent with the electrical resistivity measurement results. That is, the O_2-synthesized sample has a higher T_c and exhibits a metallic behaviour in its normal state, while the air-synthesized sample has a lower T_c and exhibits a semiconducting behaviour in its normal state.

5. Conclusion

Nearly single-phase $(Pb_{0.5}Cd_{0.5})(Sr_{0.9}Ln_{0.1})_2(Ln_{0.7}Ce_{0.3})_2Cu_2O_9$ samples have been obtained for Ln = Pr, Sm, Eu and Gd. A small amount of impurity phase exists in the Ln = Dy sample. For $(Pb_{0.5}Cd_{0.5})(Sr_{0.9}Ln_{0.1})_2(Ln_{0.7}Ce_{0.3})_2Cu_2O_9$ (Ln = Pr, Sm, Eu, Gd and Dy), the lattice parameters decrease nearly linearly with the decrease of the average ionic radius of the rare-earth element (Ln, Ce). This indicates that the crystal structure of the present compounds is very rigid. Besides this, the interplanar distance between adjacent CuO_2 planes expands as the average ionic radius of the rare-earth element (Ln, Ce) increases. The superconducting transition temperatures of these samples increase as the ionic radius of the rare-earth element Ln decreases, from Pr to Gd. The O_2-synthesized $(Pb_{0.5}Cd_{0.5})(Sr_{0.9}Gd_{0.1})_2(Gd_{0.7}Ce_{0.3})_2Cu_2O_9$ has the highest T_c-values ($T_{c,\mathrm{onset}}$ = 49 K, $T_{c,\mathrm{zero}}$ = 38 K) which, to our knowledge, are also the highest T_c-values for any 1222 phase. The superconductivity of the $(Pb_{0.5}Cd_{0.5})(Sr_{0.9}Ln_{0.1})_2(Ln_{0.7}Ce_{0.3})_2Cu_2O_9$ (Ln = Pr, Sm, Eu, Gd and Dy) system is affected by many factors. First, the decrease of the ionic radius of the rare-earth element Ln leads to the decrease of the interplanar distance between adjacent CuO_2 planes. Consequently, it strengthens the coupling effect between CuO_2 planes, and then improves the superconductivity of the present (Pb, Cd)-1222 phase. Second, the charge-carrier concentration in the CuO_2 planes also plays an important role in the superconductivity of the (Pb, Cd)-1222 phase. As the ionic radius of the rare-earth element

Ln decreases, the valence states of the Cu ions in the conducting CuO_2 planes increase. So the compounds containing smaller rare-earth elements Ln have higher carrier concentration and better superconductivity. Third, the degree of buckling of CuO_2 planes affects the superconductivity of the system, too. Going from Pr to Gd, the CuO_2 planes become flatter and flatter with the increase of the T_c-values of the corresponding samples, while the degree of buckling of the CuO_2 planes for the Ln = Dy sample begins to increase and this sample just exhibits weak superconductivity.

Acknowledgment

This work was supported by the National Centre for Research and Development on Superconductivity of China.

References

[1] Bednorz J G and Müller K A 1986 *Z. Phys.* B **64** 198
[2] Morosin B, Ginley D S, Hlava P F, Carr M J, Baughman R J, Schirber J E, Venturini E L and Kwak J F 1988 *Physica* C **152** 413
[3] Liu R S, Hervien M, Michel C, Maignan A, Martin C, Raveau B and Edwards P P 1992 *Physica* C **197** 131
[4] Cava R J, Batlogg B, Krajewski J J, Rupp L W, Schneemeyer L F, Siegrist T, Van Dover R B, Marsh P, Peck W F Jr, Gallagher P K, Glarum S H, Marshall J H, Farrow R C, Waszczak J V, Hull P and Trevor P 1988 *Nature* **336** 211
[5] Zandbergen A W, Wu W T and Van Ruitenbeek J M 1990 *Physica* C **166** 502
[6] Mochiku T, Osawa M and Asano H 1990 *Japan. J. Appl. Phys.* **29** L1406
[7] Tokiwa A, Oku T, Nagoshi M, and Syono Y 1991 *Physica* C **181** 311
[8] Tang X X and Morris D E 1991 *Phys. Rev.* B **44** 4553
[9] Tokiwa A, Oku T, Nagoshi M, Shindo D, Kikuchi M, Oikawa T, Hiraga K and Syono Y 1990 *Physica* C **172** 155
[10] Subramanian M A, Gopalakrishnan J, Torardi C C, Gai P L, Boyes D E, Askew T R, Floppen P B, Farneth W E and Sleight A W 1989 *Physica* C **157** 124
[11] Min J R, Liang J K, Chen X L, Wang C, Dong C and Rao G H 1994 *Physica* C **229** 169
[12] Min J R, Liang J K, Chen X L, Wang C, Dong C and Rao G H 1994 *Physica* C **230** 389
[13] Adachi S, Setsune K, and Wasa K 1990 *Japan. J. Appl. Phys.* **29** L890
[14] Adachi S, Inoue O, Kawashima S, Adachi H, Ichikawa Y, Setsune K and Wasa K 1990 *Physica* C **168** 1
[15] Maeda T, Sakuyama K, Koriyama S, Ichinose A, Yamauchi H and Tanaka S 1990 *Physica* C **169** 133
[16] Maeda T, Sakuyama K, Sakai N, Yamauchi H and Tanaka S 1991 *Physica* C **177** 337
[17] Maeda T, Sakai N, Izumi F, Wada T, Yamauchi H, Asano H and Tanaka S 1992 *Physica* C **193** 73
[18] Rietveld H M 1969 *J. Appl. Crystallogr.* **2** 65
[19] Brown I D 1969 *J. Solid State Chem.* **90** 155 and references therein
[20] Takahashi H, Shaked H, Hunter B A, Radaelli P G, Hitterman R L, Hinks D G and Jorgensen J D 1994 *Phys. Rev.* B **50** 3221
[21] Radaelli P G, Hinks D G, Mitchell A W, Hunter B A, Wagner J L, Dabrowski B, Vandervoort K G, Viswanathan H K and Jorgensen J D 1994 *Phys. Rev.* B **49** 4163